The IκBα/NF-κB complex has two hot spots, one at either end of the interface

SIMON BERGQVIST,[1] GOURISANKAR GHOSH, AND ELIZABETH A. KOMIVES
Department of Chemistry and Biochemistry, University of California, San Diego, La Jolla, California 92093-0378, USA
(RECEIVED July 11, 2008; FINAL REVISION August 25, 2008; ACCEPTED September 2, 2008)

Abstract

IκBα binds to and inhibits the transcriptional activity of NF-κB family members via its ankyrin repeat (AR) domain. The binding affinity of IκBα with NF-κB(p50/p65) heterodimers and NF-κB(p65/65) homodimers is in the picomolar range, and in the cell, this results in long half-lives of the complexes. Direct binding experiments have been performed using surface plasmon resonance (SPR) and isothermal titration calorimetry (ITC) on a series of truncations and mutations in order to understand what regions of the interface are most important for the tight binding affinity of this complex. We previously showed that interactions between residues 305 and 321 of NF-κB(p65) with the first AR of IκBα are critical for the binding energy. Interactions in this region are responsible for more than 7 kcal/mol of the binding energy. Here we show equally drastic consequences for the binding energy occur upon truncation of even a few residues at the C terminus of IκBα. Thus, the interface actually has two hot spots, one at either end of the elongated and large surface of interaction. These results suggest a ''squeeze'' mechanism that leads to the extremely high affinity of the IκBα•NF-κB complex through stabilization of the ankyrin repeat domain.

Keywords: protein structure/folding; specificity; PEST sequences; thermodynamics; hydrodynamics; calorimetry; kinetics; protein–protein interaction

The nuclear factor κB (NF-κB) transcription factors are activated in numerous human diseases including inflammatory and immune diseases and cancer (Kumar et al. 2004). The NF-κB family is composed of homo- and heterodimers formed from the combinatorial assembly of the p65 (RelA), RelB, c-Rel, p50, and p52 subunits, but in most cells, the most abundant NF-κB is the p50/p65 heterodimer (Ghosh et al. 1998). The inhibitor proteins IκBα, IκBβ, and IκBε bind directly to the p65 and c-Rel containing NF-κB dimers and inhibit transcriptional activity (Verma et al. 1995). In resting cells, the half-life of the NF-κB(p65) dimers bound to IκBα is on the order of days (O'Dea et al. 2008). This long half-life is consistent with the extremely large binding energy of the complex, which has a binding dissociation constant of 40 pM (Bergqvist et al. 2006). In cells, virtually no dissociation or degradation of the complex is seen in the absence of stimulation, resulting in activation of the IκB kinase, IKK, and subsequent phosphorylation at the N-terminal signal response sequence of IκBα (Karin and Ben-Neriah 2000). Phosphorylated IκBα is then ubiquitinated and degraded by the proteasome, thus freeing NF-κB to enter the nucleus, bind DNA, and activate transcription of its numerous target genes (Pahl 1999). IκB regulation of NF-κB transcriptional activity is so critical that misregulation results in many different diseases (Kumar et al. 2004). In fact, constitutive activation of NF-κB is observed in many types of cancer, and improper IκBα function is observed in B-cell and Hodgkin's lymphomas (Lee et al. 2007).

In contrast to its remarkable stability in the NF-κB-bound state, free IκBα is intrinsically unstable, its half-life is <10

[1]Present address: Department of Biochemical Pharmacology, Pfizer Global Research and Development, San Diego, CA 92121, USA.
Reprint requests to: Elizabeth A. Komives, Department of Chemistry and Biochemistry, University of California, San Diego, 9500 Gilman Drive, La Jolla, California 92093-0378, USA; e-mail: ekomives@ucsd.edu; fax: (858) 534-6174.
Article and publication are at http://www.proteinscience.org/cgi/doi/10.1110/ps.037481.108.

min, and it is rapidly degraded in a process that does not require phosphorylation or ubiquitination (Krappmann et al. 1996; Mathes et al. 2008). These distinct degradation pathways for free and NF-κB-bound IκBα appear to be critical for signal-responsive NF-κB activation. Decreases in NF-κB-bound IκBα phosphorylation reduce NF-κB activation upon stimulation in a mathematical model of NF-κB signaling (O'Dea et al. 2007). Furthermore, IκBα variants with slower basal degradation rates result in slower activation of NF-κB upon stimulation with TNF-α (Mathes et al. 2008). Thus, in resting cells, continual synthesis and rapid degradation of IκBα tightly inhibits NF-κB activity, while allowing a rapid response to external stimuli. An important goal of the present work is to understand how binding to NF-κB stabilizes IκBα, and how the binding energy of this complex is established.

IκBα is composed of an N-terminal signal response region where phosphorylation and ubiquitination occur, an ankyrin repeat (AR) domain that binds to NF-κB (Fig. 1A), and a C-terminal PEST sequence (Huxford et al. 1998; Jacobs and Harrison 1998). ARs are 30–40-amino-acid repeating sequences composed of a β-hairpin followed by two antiparallel α-helices and a variable loop. ARs are found in more than 3000 different proteins with highly varied functions (Mosavi et al. 2004). AR domains contain multiple ARs and function by mediating specific protein–protein interactions (Li et al. 2006). Statistical analysis of AR sequences revealed a consensus sequence, and consensus AR repeat domains are highly stable compared with their natural counterparts (Barrick et al. 2008).

All six IκBα ARs contact NF-κB, and the IκBα•NF-κB interface buries more than 4000 Å^2 of surface area (Fig. 1A; Huxford et al. 1998; Jacobs and Harrison 1998). Characterization of IκBα reveals that ARs 5 and 6 are weakly folded and highly dynamic, but they fold upon binding to NF-κB (Croy et al. 2004; Truhlar et al. 2006; Ferreiro et al. 2007). In previous work, we truncated the N and C termini of NF-κB(p65) and found an energetic hot spot (Bergqvist et al. 2006). The concept of ''hot spots'' in protein–protein interfaces was first described by Wells and colleagues, who used alanine scanning mutagenesis to determine which residues at the interface of the human growth hormone interface with its receptor were important for the binding interaction energy (Clackson and Wells 1995). Although many residues made contacts at the interface, few of these contacts were actually important for the binding energy. Similarly, mutation of the contacting residues in much of the IκBα•NF-κB interface had little effect on the binding energy (Huxford et al. 2002). We previously reported a binding energy hot spot at one end of the elongated interface, where helix 4 (or NLS extension) of the NF-κB p65 Rel-homology region (residues 305–321) contacts the first ankyrin repeat of IκBα, the NLS hot spot. Truncation of residues 305–321 in NF-κB p65 dramatically weakened the binding interaction, increasing the K_D 5000-fold (Bergqvist et al. 2006). The biological relevance of this result is that the NLS hot spot, which involves residues 305 and 321 in NF-κB p65, anchors the NLS, which is effectively sequestered in the complex by IκBα (Baeuerle and Baltimore 1988).

In experiments presented here, we demonstrate the existence of a second hot spot, at the opposite end of the elongated interface where the IκBα PEST sequence contacts the dimerization domain of NF-κB(p65). This hot spot will be referred to as the ''PEST hot spot.'' The results show that whereas truncation of the residues C-terminal to the PEST sequence (residues 288–317) had no effect on binding affinity, truncation of the PEST sequence itself (residues 276–287) reduced binding more than 500-fold.

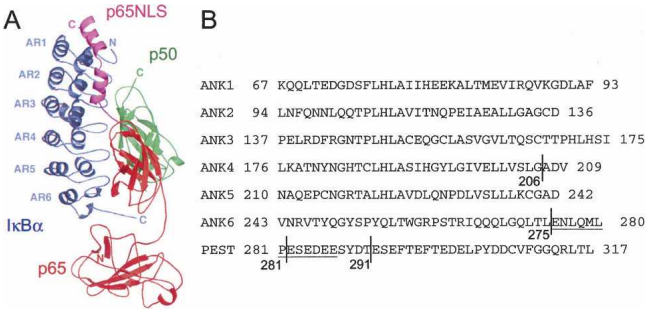

Figure 1. (*A*) The crystal structure of (blue) IκBα bound to NF-κB; (green) p50; (red) p65; PDB accession number 1NFI (Jacobs and Harrison 1998). Figure prepared using PyMOL (DeLano Scientific). (*B*) The sequences of the IκBα ankryin repeats (ARs) are aligned with the consensus sequence for a stable AR (Mosavi et al. 2002). Vertical lines indicate truncations used in this study. The PEST sequence is underlined.

Results

C-terminal truncation of IκBα

To understand the role of the C terminus of IκBα in binding NF-κB, the protein was truncated at several positions by site-directed mutagenesis to introduce a stop codon (Fig. 1B). The crystal structure of IκBα in complex with NF-κB(p50/p65), solved in two different laboratories using slightly different truncated forms of each protein, was used as a guide. Huxford et al. (1998) used IκBα (67–302), while Jacobs and Harrison (1998) used IκBα (67–287). In the crystal structure containing IκBα (67–302), no electron density was observed for residues 292–302, but truncation of IκBα at residue 291 resulted in a protein that aggregated and could not be produced in monomeric form. Several of the other truncation mutants also had a high propensity for aggregation. The IκBα (67–287), IκBα (67–281), IκBα

(67–275), and IκBα (67–206) proteins were expressed and purified in sufficient quantities for SPR and ITC experiments. IκBα (67–281) could not be concentrated to the same extent as the others and so was only used for surface plasmon resonance (SPR).

SPR binding experiments

The binding kinetics of each of the truncated forms of IκBα were characterized by SPR. The experimental protocol used the Rel-homology domain of p65, which had been mutated to introduce a single cysteine at the N terminus that was subsequently biotinylated. The biotinylated p65 protein was captured on a streptavidin (SA) SPR chip. This surface was stable and could be regenerated after each binding experiment using urea as previously described (Bergqvist et al. 2006). Sensorgrams for IκBα (67–287) binding to NF-κB shown in Figure 2A reveal that IκBα (67–287) binds tightly to NF-κB. The association rate is rapid, and the dissociation rate is slow (10^{-4} s^{-1}). The binding kinetics and thermodynamics of IκBα (67–287) as compared to IκBα (67–317) were identical (Table 1A).

Truncation of even part of the PEST sequence resulted in a drastic loss of binding affinity. IκBα (67–281), which is only six residues shorter, had a 60-fold (2.5 kcal/mol) weaker binding affinity, an effect that was mainly due to an increased dissociation rate (Fig. 2B; Table 1A). Further truncation to produce IκBα (67–275) resulted in a protein with a K_D that was more than 500-fold weaker than that of the full-length protein (Fig. 2C; Table 1A).

The binding affinity of IκBα (67–287) to NF-κB($p50_{(248–350)}$/$p65_{(190–321)}$), which is missing the N-terminal domain of p65, was eightfold lower in affinity than binding to NF-κB($p50_{(248–376)}$/$p65_{(19–325)}$). Again, the truncations substantially weakened the binding (Fig. 3; Table 1). Kinetic constants for binding could not be obtained for IκBα (67–275) at 37°C because of the rapid dissociation rate; however, comparison of the binding of IκBα (67–275) to NF-κB($p50_{(248–376)}$/$p65_{(19–325)}$) at 37°C and 25°C shows a sevenfold higher binding affinity at the lower temperature (Table 1). Thus, in the absence of the p65 N-terminal domain, truncation of the PEST sequence resulted in a 250-fold (3.8 kcal/mol) decrease in binding affinity.

Phosphorylation of IκBα PEST sequence is not critical for tight binding

Since truncation of IκBα PEST sequence identified residues that were critical for binding, the effect of phosphorylation of these residues on the binding kinetics was investigated. IκBα(67–317) was incubated at either

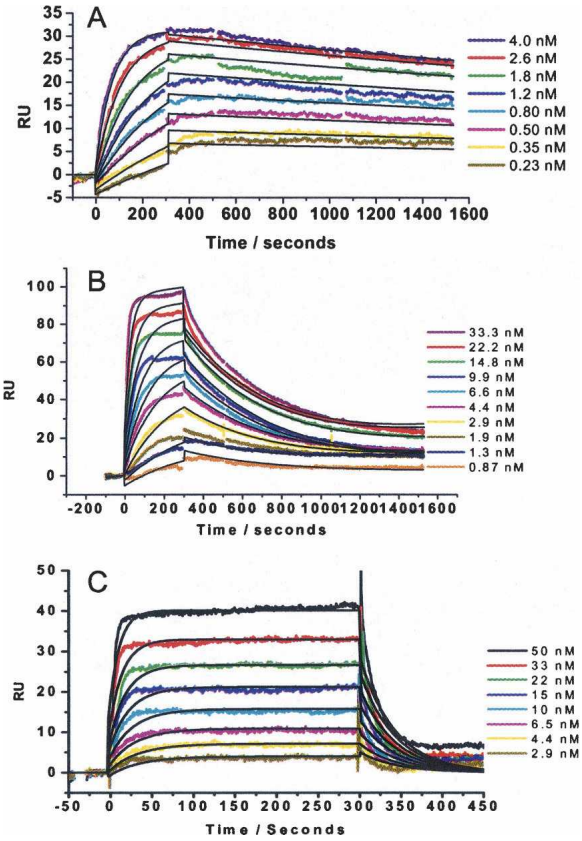

Figure 2. SPR data collected for the truncated IκBα proteins interacting with NF-κB($p50_{248–376}$/$p65_{19–325}$). In all experiments, the NF-κB was immobilized to a streptavidin chip by a biotin tag on the p65 N terminus, and IκBα was flowed over at a flow rate of 50 μL per minute. (*A*) Sensorgrams of 0.23 to 4.0 nM IκBα(67–287) flowed over NF-κB($p50_{248–376}$/$p65_{19–325}$) at 37°C. (*B*) Sensorgrams of 0.87 to 33 nM IκBα(67–281) flowed over NF-κB($p50_{248–376}$/$p65_{19–325}$) at 37°C. (*C*) Sensorgrams of 2.9 to 50 nM IκBα(67–275) flowed over NF-κB($p50_{248–376}$/$p65_{19–325}$) at 37°C.

37°C or 25°C for different periods of time with casein kinase II, which was known from previous work to phosphorylate the PEST sequence of IκBα (Phelps et al. 2000). Since we previously reported that incubation at 37°C causes aggregation of IκBα (Croy et al. 2004), the protein was purified after phosphorylation by size exclusion chromatography, the monomer was collected, and the concentration was re-determined. The binding affinity was slightly improved by phosphorylation, owing to an increase in the association rate of the phosphorylated protein (Table 1B).

ITC binding experiments

To further investigate the thermodynamics of binding, isothermal titration calorimetry (ITC) experiments were performed. Only three of the proteins could be obtained at

Table 1. *SPR kinetic values for interactions between NF-κB and IκB constructs*

A. Interaction of NF-κB($p50_{248–376}$/$p65_{19–325}$)[a] with truncated IκBαs

Interaction[a]	NF-κB[a]	Temperature (°C)	k_a ($\times 10^6$ M^{-1} s^{-1})	k_d ($\times 10^{-4}$ s^{-1})	$K_{D,obs}$ ($\times 10^{-11}$ M^{-1})	ΔG (kcal/mol)
IκBα (67–317)	FL	37	3.3 ± 0.6	1.4 ± 0.55	4.5 ± 1.0	−14.68
IκBα (67–287)	FL	37	3.7 ± 0.10	1.5 ± 0.14	3.9 ± 0.3	−14.77
IκBα (67–281)	FL	37	0.9 ± 0.3	22 ± 0.8	247 ± 16	−12.21
IκBα (67–275)	FL	37	1.9 ± 1.0	398 ± 220	2070 ± 100	−10.90
IκBα (67–275)	FL	25	1.6 ± 0.1	48 ± 2.0	300 ± 20	−11.63
IκBα (67–287)	dd	37	1.7 ± 0.32	5.4 ± 1.0	32 ± 10	−13.47
IκBα (67–281)	dd	37	1.2 ± 0.4	61.8 ± 12	556 ± 78	−11.71
IκBα (67–275)	dd	25	1.5 ± 0.3	180 ± 12	1200 ± 100	−10.80

B. Effects of PEST phosphorylation on the interaction of NF-κB($p50_{248-350}$/$p65_{190-321}$) with IκBα

Interaction	Temperature (°C)	k_a ($\times 10^6$ M^{-1} s^{-1})	k_d ($\times 10^{-4}$ s^{-1})	$K_{D,obs}$ ($\times 10^{-10}$ M^{-1})	ΔG (kcal/mol)
IκBα (67–287)	37	1.7 ± 0.3	5.4 ± 0.1	3.2 ± 0.1	−13.47
IκBα (67–317p)[b]	37	7.8 ± 0.8	10.9 ± 0.7	1.4 ± 0.08	−13.98

[a] FL denotes NF-κB($p50_{248–376}$/$p65_{19–325}$); dd denotes NF-κB($p50_{248–350}$/$p65_{190–321}$), where the p65 was specifically biotinylated and immobilized.
[b] IκBα (67–317p) containing the full PEST sequence was phosphorylated with casein kinase II and then repurified by size exclusion chromatography.

sufficiently high concentrations for these experiments. The ITC results confirm that the binding of IκBα (67–287) is very tight, too tight, in fact, to measure the K_D and therefore the ΔG accurately by ITC (Fig. 4A; Table 2). Stoichiometric binding was observed from which only the ΔH_{obs} was determined. This result was consistent with the binding affinity of 40 pM determined previously by SPR (Bergqvist et al. 2006). The binding affinity was similar for IκBα (67–287) binding to NF-κB(p65/p65), although the ΔH_{obs} was somewhat more favorable (Fig. 4B; Table 2). As was seen in the SPR experiments, truncation of as few as 12 residues resulted in a drastic loss of binding energy (Table 2). Almost all of the decrease in ΔG can be attributed to a loss of favorable enthalpy of binding (Fig. 4C). Further truncation to produce IκBα (67–206) resulted in a further reduction in the ΔH_{obs} (Fig. 4D). The binding energy of IκBα (67–206) is contributed almost equally by favorable changes in enthalpy and entropy.

Discussion

The IκBα PEST sequence provides a second hot spot in the NF-κB binding interface

Amide $H/^2H$ exchange experiments on IκBα (67–317) and (67–287) revealed that the PEST sequence is completely solvent-accessible (Croy et al. 2004; Truhlar et al. 2006). These experiments also revealed that the fifth and sixth ARs near the C-terminal part of IκBα fold upon binding to NF-κB. In order to ascertain whether the C terminus of IκBα was important for the binding energy, various truncations of IκBα were made. The results presented here show that the IκBα•NF-κB binding interface has a second hot spot where the IκBα PEST sequence interacts with the dimerization domain of p65. Deletion of the PEST extension (residues 288–317) had no effect on the binding affinity, but deletion of the PEST itself (residues 276–287) caused more than a 500-fold decrease in binding affinity. This ''PEST hot spot'' helps explain the very high affinity observed for the IκBα•NF-κB interaction.

This observation is significant for understanding the mechanism of control of degradation of IκBα (Fig. 5). The rates of degradation of free versus bound IκBα are critical parameters in the way in which the NF-κB signaling module functions (O'Dea et al. 2007). Free IκBα has an intracellular half-life of <10 min and is degraded by a ubiquitin-independent mechanism that depends on certain residues within the PEST sequence (Mathes et al. 2008). In contrast, NF-κB-bound IκBα is extremely stable and appears to only be degraded if the N-terminal domain of IκBα is phosphorylated and ubiquitinated in a signal-dependent manner (O'Dea et al. 2007). Thus, for NF-κB binding to completely inhibit the ubiquitin-independent proteasome degradation of IκBα, it must effectively sequester the PEST sequence. The results presented here suggest that, indeed, tight binding of the IκBα PEST sequence by NF-κB may be part of the control mechanism.

It is interesting that phosphorylation of the PEST sequence does not seem to markedly increase binding, but, rather, it simply increases the association rate and has only a minor effect on the observed dissociation rate. Phosphorylation of the IκBα PEST sequence may increase the electrostatic steering component of the

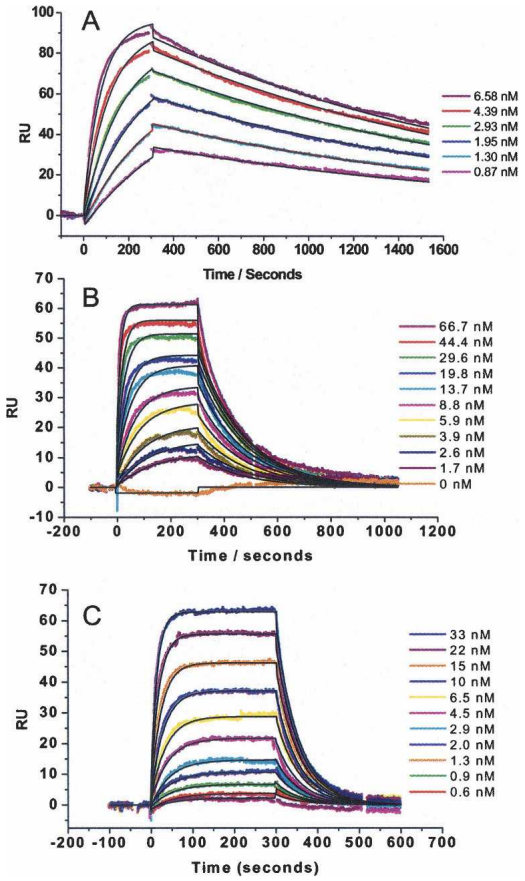

Figure 3. SPR data collected for the truncated IκBα proteins interacting with NF-κB($p50_{248–350}$/$p65_{190–321}$). In all experiments, the NF-κB was immobilized to a streptavidin chip by a biotin tag on the p65 N terminus, and IκBα was flowed over at a flow rate of 50 μL per minute. (*A*) Sensorgrams of 0.87 to 6.58 nM IκBα(67–287) flowed over NF-κB($p50_{248–350}$/$p65_{190–321}$) at 37°C. (*B*) Sensorgrams of 1.73 to 66.7 nM IκBα(67–281) flowed over NF-κB($p50_{248–350}$/$p65_{190–321}$) at 37°C. (*C*) Sensorgrams of 0.58 to 33 nM IκBα(67–275) flowed over NF-κB($p50_{248–350}$/$p65_{190–321}$) at 25°C.

encounter complex, leading to a significant increase in the association rate (Baerga-Ortiz et al. 2000).

The "fold and squeeze" mechanism of IκBα•NF-κB binding

The NLS hot spot involves the first three ARs of IκBα, which are well-folded interacting with the NLS of NF-κB(p65), which is not well-folded. Theoretical studies strongly suggest that the NLS sequence folds upon binding (Lätzer et al. 2007), and NMR evidence supports this idea (C.F. Cervantes and E.A. Komives, unpubl.). The PEST hot spot involves the folded dimerization domain of NF-κB interacting with the PEST of IκBα, which is not well-folded. Amide $H/^2H$ exchange monitored by mass spectrometry showed that the C-terminal residues of IκBα are fully exchanged within 30 sec (Croy et al. 2004), but crystallography and NMR show that this part of the protein is at least partly structured in the bound complex (Huxford et al. 1998; Sue et al. 2008). Thus, the NLS hot spot involves a folded part of IκBα interacting with a partially unfolded part of NF-κB, and the PEST hot spot involves a partially unfolded part of IκBα interacting with a folded part of NF-κB. Thus, both hot spots appear to involve folding coupled to binding.

The fact that the ends of the interface were critically important for binding, whereas mutation of interface residues in the middle of the interface had no effect, hinted at the possibility of a "squeeze" mechanism of complex formation. In this mechanism, binding energy would be gained through folding of the IκBα AR domain upon binding. It is now known that the contacts between ankyrin

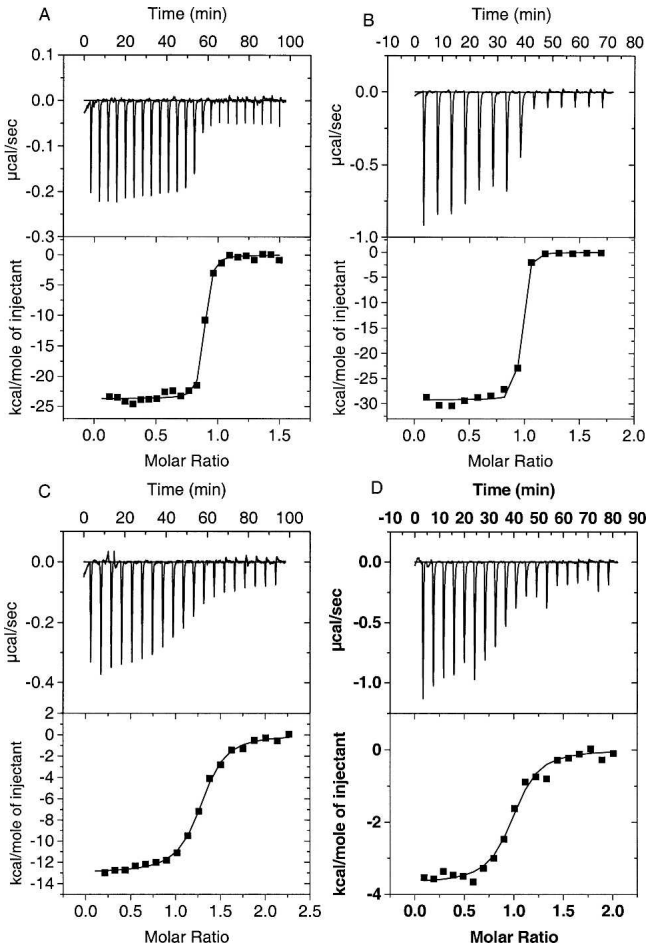

Figure 4. ITC binding isotherms for NF-κB binding to truncated IκBα in 150 mM NaCl, 10 mM MOPS, pH 7.5, 0.5 mM EDTA, and 0.5 mM sodium azide at 30°C. Data were analyzed using a model for a single set of identical binding sites after the heats of dilution of NF-κB into buffer were subtracted. (*A*) IκBα(67–287) binding to NF-κB($p50_{248–350}$/$p65_{190–321}$). (*B*) IκBα(67–287) binding to NF-κB($p65_{190–321}$/$p65_{190–321}$). (*C*) IκBα(67–275) binding to NF-κB($p65_{190–321}$/$p65_{190–321}$). (*D*) IκBα(67–206) binding to NF-κB($p50_{248–350}$/$p65_{190–321}$).

Table 2. *Thermodynamic data for IκBα variants to NF-κB*[a] *by ITC*

IκBα	Temperature (°C)	NF-κB	ΔH	$-T\,\Delta S$	$K_{D,obs}$ ($\times 10^{-9}$ M^{-1})	ΔG (kcal/mol)
IκBα (67–287)	30°C	p50/p65	−23.7 ± 0.19	ND	<2.2[b]	ND
IκBα (67–287)	35°C	p50/p65	−31.6 ± 0.26	ND	<2.2[b]	ND
IκBα (67–287)	30°C	p65/p65	−29.2 ± 0.29	ND	<1.8	ND
IκBα (67–275)	30°C	p50/p65	ND			
IκBα (67–275)	30°C	p65/p65	−13.0 ± 0.11	3.1	69.4 ± 6.5	−9.9
IκBα (67–206)	30°C	p50/p65	−3.8 ± 0.07	−4.2	1690 ± 220	−8.0
IκBα (67–206)	30°C	p65/p65	ND			

[a] p50/p65 is NF-κB($p50_{248–350}$/$p65_{190–321}$), and p65 is the $p65_{190–321}$ homodimer.
[b] For these complexes, we observed stoichiometric binding. Assuming a maximal *c*-value of 1000 as defined by Wiseman et al. (1989), the lower limit for the K_D is 3 nM.

repeats are most important in establishing the folding energy of AR domains, and thus it seemed possible that additional energy could be gained by ''squeezing'' the IκBα AR domain at either end. In fact, the fifth and sixth repeats of IκBα are known to fold upon binding (Truhlar et al. 2006). This is consistent with the very large ΔH_{obs}, of −31.6 kcal/mol at 35°C (Table 2) and with the large observed heat capacity change reported previously (Bergqvist et al. 2006). The ΔG determined from the SPR binding is −14.7 kcal/mol at 37°C, and therefore the entropy change upon binding is large and negative. The ΔH_{obs} is strongly temperature dependent, so that at 25°C the ΔH_{obs} is −15.1 kcal/mol, and the entropy change is much smaller relative to ΔG ($T\Delta S$ = +1.9 kcal/mol) (Bergqvist et al. 2006). Owing to the multiple and complex interplay of coupled folding upon binding events, it is difficult to generalize the interpretation of the thermodynamic information.

Recently completed NMR experiments on the IκBα•NF-κB complex provide evidence for the ''squeeze'' mechanism. Cross-peaks for residues in the third AR of IκBα appear well-folded in the free AR domain, but disappear when IκBα is bound to NF-κB (Sue et al. 2008). The disappearance of cross-peaks in the NMR is a strong indicator of backbone dynamics in the millisecond time regime and often indicates motional averaging. Thus, the well-folded middle of the IκBα AR domain appears to become more disordered in the complex, perhaps partially compensating for the entropy cost of folding upon binding. It is possible that protein–protein interactions mediated by AR domains may have multiple ways of achieving binding specificity and affinity, one of which involves gaining binding energy from internal AR domain stabilization as in the ''squeeze'' mechanism.

Materials and Methods

Protein expression and purification

Human IκBα (67–287) was expressed in the Pet 11a vector and purified as previously described (Croy et al. 2004). Full-length NF-κB($p50_{(248–376)}$/$p65_{(19–325)}$) was produced by coexpression using a Pet 11a single expression vector and purified using a tandem column technique. Cells were harvested and sonicated. The lysate was then centrifuged at 12,000 rpm for 45 min, and the supernatant was loaded onto a tandem fast flow Q and fast flow S column (GE Healthcare) equilibrated in 50 mM NaCl, 25 mM Tris, pH 7.5, and 0.5 mM EDTA. After loading, the Q column was disconnected, and protein fractions were eluted from the S with a gradient from 50 to 400 mM NaCl. Fractions were collected and analyzed by SDS-PAGE with visualization by silver staining. The final step of the purification was size exclusion on an S-200 Superdex column equilibrated in 150 mM NaCl, 10 mM MOPS, pH 7.5, 0.5 mM EDTA, and 0.5 mM sodium azide.

For the NF-κB $p65_{190–321}$ and NF-κB $p50_{248–350}$ constructs, *E. coli* BL21 DE3 cells were grown to an OD of 0.6 and induced at room temperature for 16 h with 0.1 mM IPTG. For the NF-κB $p65_{190–321}$, the tandem column was equilibrated in 50 mM NaCl, 25 mM MES pH 7.0, 10 mM BME, and 0.5 mM EDTA; and for the NF-κB $p50_{248–350}$, the tandem column was equilibrated in 50 mM NaCl, 25 mM MES pH 6.2, 10 mM BME, and 0.5 mM EDTA, and a gradient of 50–300 mM NaCl was run. For the NF-κB $p65_{1–325}$, NF-κB $p65_{1–304}$ and NF-κB $p50_{39–363}$ proteins, cells were induced with 0.5 mM IPTG. For NF-κB $p65_{1–325}$, the tandem column was equilibrated in 50 mM NaCl, 25 mM MES pH 6.5, 10 mM BME, and 0.5 mM EDTA, and the gradient was 50–450 mM NaCl. For NF-κB $p65_{1–304}$, the tandem column was equilibrated in 50 mM NaCl, 25 mM Tris, pH 7.0, 10 mM BME,

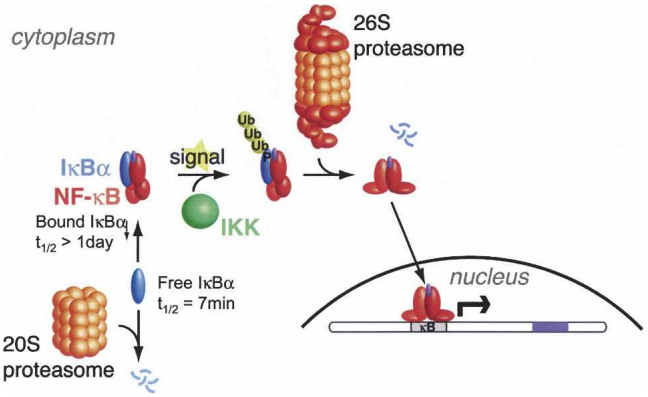

Figure 5. Schematic representation of the IκBα degradation pathways showing the various rates of degradation.

and 0.5 mM EDTA, and a 50–300 mM gradient was used. For NF-κB $p50_{39–363}$, the tandem column was equilibrated in 50 mM NaCl, 25 mM MES, pH 6.2, 10 mM BME, and 0.5 mM EDTA, and the gradient was from 50 to 700 mM NaCl.

Protein concentrations were determined spectrophotometrically using the following ε_{280} values: 24,180 for NF-κB $p50_{248–350}$, 21,620 for NF-κB $p65_{190–321}$, 19,060 for NF-κB $p65_{190–304}$, 36,980 for NF-κB $p65_{1–325}$, 34,420 for NF-κB $p65_{1–325}$, 42,100 for NF-κB $p50_{39–363}$ homodimers, 30,580 for NF-κB($p50_{248–376}$/$p65_{19–325}$), 22,900 for NF-κB($p50_{248–350}$/$p65_{190–321}$), 21,620 for NF-κB($p50_{248–350}$/$p65_{190–304}$), 39,540 for NF-κB($p50_{39–363}$/$p65_{1–325}$), and 38,260 for NF-κB($p50_{39–363}$/$p65_{1–304}$) heterodimers. For $I\kappa B\alpha_{67–287}$, an ε_{280} of 12,090 was used. For ITC experiments, dimers were formed in vitro by incubating an equimolar amount for 2 h at 25°C and overnight at 4°C. For SPR experiments, the purified fractions of NF-κB($p50_{(248–376)}$/$p65_{(19–325)}$) were biotinylated by incubation with a 1:1 molar ratio of biotin PEO maleimide (Pierce Chemicals), for 30 min at room temperature, and purified immediately by size exclusion chromatography on an S200 Superdex 16/60 column. Fractions containing the biotinylated heterodimer were collected and stored at −80°C in 50-μL portions until captured on a streptavidin (SA) SPR chip.

SPR experiments

Sensorgrams were recorded on a Biacore 3000 instrument using streptavidin (SA) chips. Biotinylated NF-κB was immobilized on the chip in a high-salt buffer (500 mM NaCl, 10 mM Tris, pH 7.5, 0.5 mM EDTA, 0.5 mM sodium azide, 0.005% P20). Sensorgrams were run in the automatic subtraction mode using flow cell 1 (FC 1) as an unmodified reference. Data were collected for FCs 2, 3, and 4, which contained varying amounts of NF-κB bound with the lowest amount immobilized on FC2 (200 RU) and the highest on FC4 (400 RU). Sensorgrams were recorded using several ranges of IκBα depending on the binding affinity of the complex. Injections were made using the kinject injection mode, alternating highest with lowest concentration samples, with a 5-min contact time and a 1200-sec dissociation phase in all cases, except for the weaker interactions, where a 3-min contact time and a 3-min dissociation phase were used. The running buffer used for the binding experiments was 150 mM NaCl, 10 mM Tris, pH 7.5, 10% (w/v) glycerol, 3 mM DTT, 0.5 mM sodium azide, 0.2 mM EDTA, and 0.005% P20. The glycerol improved the stability of the NF-κB during regeneration. Regeneration was achieved using a 1-min pulse of a urea solution. The concentration of urea required depended on the NF-κB construct and the experimental temperature and was prepared by diluting a 6 M stock into the running buffer. The minimum urea concentration required for complete regeneration under each condition was determined by repeat injections. The data were analyzed using the Bia Evaluation 4.1 software with a simple 1:1 Langmuir binding model. Between three and 12 sensorgrams were obtained for each construct and condition tested using a range of immobilized NF-κB and IκBα concentrations. For the weaker interactions, data were also analyzed by equilibrium analysis in addition to the kinetic analysis. The equilibrium response was plotted against the IκBα concentration, and a line was fit to $R = K_A[I\kappa B\alpha] \times R_{max}/(K_A[I\kappa B\alpha] + 1)$, where R is the equilibrium response at a specific IκBα concentration, R_{max} is the response at saturation of the ligand on the chip, and $K_A = 1/K_D$.

ITC experiments

ITC experiments were carried out on a Microcal MCS instrument. IκBα and NF-κBs were purified by size exclusion chromatography on an S-75 or S-200 column, respectively, immediately prior to use. In a typical ITC experiment, 20 15-μL injections of 50 μM NF-κB were made into a 5 μM IκBα solution in the cell. ITC experiments were carried out in a buffer of 150 mM NaCl, 10 mM MOPS, pH 7.5, 0.5 mM EDTA, and 0.5 mM sodium azide. Isotherms were analyzed using Origin software (Microcal) as described elsewhere (Bergqvist et al. 2004). For the very tight complexes, we observed stoichiometric binding assuming a maximal *c*-value of 1000 as defined by Wiseman et al. (1989); the lower limit for the K_D is 3 nM.

Acknowledgment

Research funding was provided by NIH grant GM071862.

References

Baerga-Ortiz, A., Rezaie, A.R., and Komives, E.A. 2000. Electrostatic dependence of the thrombin–thrombomodulin interaction. *J. Mol. Biol.* **296:** 651–658.

Baeuerle, P.A. and Baltimore, D. 1988. IκB: A specific inhibitor of the NF-κB transcription factor. *Science* **242:** 540–546.

Barrick, D., Ferreiro, D.U., and Komives, E.A. 2008. Folding landscapes of ankyrin repeat proteins: Experiments meet theory. *Curr. Opin. Struct. Biol.* **18:** 27–34.

Bergqvist, S., Williams, M.A., O'Brien, R., and Ladbury, J.E. 2004. Heat capacity effects of water molecules and ions at a protein–DNA interface. *J. Mol. Biol.* **336:** 829–842.

Bergqvist, S., Croy, C.H., Kjaergaard, M., Huxford, T., Ghosh, G., and Komives, E.A. 2006. Thermodynamics reveal that helix four in the NLS of NF-κB p65 anchors IκBα, forming a very stable complex. *J. Mol. Biol.* **360:** 421–434.

Clackson, T. and Wells, J.A. 1995. A hot spot of binding energy in a hormone-receptor interface. *Science* **267:** 383–386.

Croy, C.H., Bergqvist, S., Huxford, T., Ghosh, G., and Komives, E.A. 2004. Biophysical characterization of the free IκBα ankyrin repeat domain in solution. *Protein Sci.* **13:** 1767–1777.

Ferreiro, D.U., Cervantes, C.F., Truhlar, S.M., Cho, S.S., Wolynes, P.G., and Komives, E.A. 2007. Stabilizing IκBα by "consensus" design. *J. Mol. Biol.* **365:** 1201–1216.

Ghosh, S., May, M.J., and Kopp, E.B. 1998. NF-κB and Rel proteins: Evolutionarily conserved mediators of immune responses. *Annu. Rev. Immunol.* **16:** 225–260.

Huxford, T., Huang, D.B., Malek, S., and Ghosh, G. 1998. The crystal structure of the IκBα/NF-κB complex reveals mechanisms of NF-κB inactivation. *Cell* **95:** 759–770.

Huxford, T., Mishler, D., Phelps, C.B., Huang, D.B., Sengchanthalangsy, L.L., Reeves, R., Hughes, C.A., Komives, E.A., and Ghosh, G. 2002. Solvent exposed non-contacting amino acids play a critical role in NF-κB/IκBα complex formation. *J. Mol. Biol.* **324:** 587–597.

Jacobs, M.D. and Harrison, S.C. 1998. Structure of an IκBα/NF-κB complex. *Cell* **95:** 749–758.

Karin, M. and Ben-Neriah, Y. 2000. Phosphorylation meets ubiquitination: The control of NF-κB activity. *Annu. Rev. Immunol.* **18:** 621–663.

Krappmann, D., Wulczyn, F.G., and Scheidereit, C. 1996. Different mechanisms control signal-induced degradation and basal turnover of the NF-κB inhibitor IκBα in vivo. *EMBO J.* **15:** 6716–6726.

Kumar, A., Takada, Y., Boriek, A.M., and Aggarwal, B.B. 2004. Nuclear factor-κB: Its role in health and disease. *J. Mol. Med.* **82:** 434–448.

Lätzer, J., Papoian, G.A., Prentiss, M.C., Komives, E.A., and Wolynes, P.G. 2007. Induced fit, folding, and recognition of the NF-κB-nuclear localization signals by IκBα and IκBβ. *J. Mol. Biol.* **367:** 262–274.

Lee, C.H., Jeon, Y.T., Kim, S.H., and Song, Y.S. 2007. NF-κB as a potential molecular target for cancer therapy. *Biofactors* **29:** 19–35.

Li, J., Mahajan, A., and Tsai, M.D. 2006. Ankyrin repeat: A unique motif mediating protein–protein interactions. *Biochemistry* **45:** 15168–15178.

Mathes, E., O'Dea, E.L., Hoffmann, A., and Ghosh, G. 2008. NF-κB dictates the degradation pathway of IκBα. *EMBO J.* **27:** 1357–1367.

Mosavi, L.K., Minor Jr., D.L., and Peng, Z.Y. 2002. Consensus-derived structural determinants of the ankyrin repeat motif. *Proc. Natl. Acad. Sci.* **99:** 16029–16034.

Mosavi, L.K., Cammett, T.J., Desrosiers, D.C., and Peng, Z.Y. 2004. The ankyrin repeat as molecular architecture for protein recognition. *Protein Sci.* **13:** 1435–1448.

O'Dea, E.L., Barken, D., Peralta, R.Q., Tran, K.T., Werner, S.L., Kearns, J.D., Levchenko, A., and Hoffmann, A. 2007. A homeostatic model of IκB metabolism to control constitutive NF-κB activity. *Mol. Syst. Biol.* **3:** 111. doi: 10.1038/msb4100148.

O'Dea, E.L., Kearns, J.D., and Hoffmann, A. 2008. UV as an amplifier rather than inducer of NF-κB activity. *Mol. Cell* **30:** 632–641.

Pahl, H.L. 1999. Activators and target genes of Rel/NF-κB transcription factors. *Oncogene* **18:** 6853–6866.

Phelps, C.B., Sengchanthalangsy, L.L., Huxford, T., and Ghosh, G. 2000. Mechanism of IκBα binding to NF-κB dimers. *J. Biol. Chem.* **275:** 29840–29846.

Sue, S.C., Cervantes, C., Komives, E.A., and Dyson, H.J. 2008. Transfer of flexibility between ankyrin repeats in IκBα upon formation of the NF-κB complex. *J. Mol. Biol.* **380:** 917–931.

Truhlar, S.M., Torpey, J.W., and Komives, E.A. 2006. Regions of IκBα that are critical for its inhibition of NF-κB•DNA interaction fold upon binding to NF-κB. *Proc. Natl. Acad. Sci.* **103:** 18951–18956.

Verma, I.M., Stevenson, J.K., Schwarz, E.M., Van Antwerp, D., and Miyamoto, S. 1995. Rel/NF-κB/IκB family: Intimate tales of association and dissociation. *Genes & Dev.* **9:** 2723–2735.

Wiseman, T., Williston, S., Brandts, J.F., and Lin, L.N. 1989. Rapid measurement of binding constants and heats of binding using a new titration calorimeter. *Anal. Biochem.* **179:** 131–137.